Computational Approach to Investigating Electronic Transport in Graphene Multibarrier Structures

M. Miniya[1][0000−0002−5184−4938], Y. Rodríguez-Lazcano[1][0000−0002−8488−9518], David Quesada Saliba[2][0000−0001−8211−6485], and Luis Manuel Gaggero Sager[3][0000−0002−4232−6346]

[1] Unidad Académica de Ciencias Básicas e Ingeniería, Universidad Autónoma de Nayarit, 63155 Tepic, Nayarit

[2] Computational Clinical Systems Biology Group, INIM, Kiran Patel College Osteopathic Medicine, Nova Southeastern University, Ft. Lauderdale/Davie, FL 33314-7796, USA

[3] Centro de Investigación en Ingeniería y Ciencias Aplicadas, Universidad Autónoma del Estado de Morelos, Avenida Universidad 1001, cd48, Chamilpa, 62209 Cuernavaca, Morelos, México

Abstract. Numerical study of electronic transport in graphene-based structures with electrostatic multipotentials. A mathematical model based on the transfer matrix formalism was employed, implemented through an algorithm to calculate the transmission coefficient and conductance for different multibarrier structure in a graphene monolayer. The results show that the number of barriers, the dimensions of the barriers, and the angle of incidence significantly affect the physical properties of graphene. These findings open perspectives for experimentalists to develop electronic devices.

Keywords: Electronic transport · Graphene · Superlattice · Numerical study.

1 Introduction

Computational methods play a fundamental role in modern physics [1, 2], enabling the simulation, modeling, and analysis of complex systems that are often inaccessible through purely analytical approaches or experimental techniques. These methods are used across various subfields, including condensed matter physics [3], and materials science [4], enabling for instance, both qualitative and quantitative studies of transport properties of materials such as graphene.

Graphene is a two-dimensional material based on carbon atoms which are arranged in an hexagonal crystalline lattice, and behaves as a conductor [5, 6]. It possesses many remarkable and exotic properties, which have been the subject of extensive research. Notable among these are the Klein tunneling phenomenon, the Hall effect, and others [7, 8]. However, controlling electrons in graphene has also been extensively investigated. One of the methods used to this end, involves

https://doi.org/10.61728/AE20254957

applying electrostatic potentials or using substrates, which have proven to be key tools for modulating the band structure, redistributing the density of states, and creating energy regions with accumulated energy levels [9–11] Since the discovery of graphene, it has opened the door to countless possibilities for applications in various fields. Numerous prototypes of transistors, sensors, and batteries have been developed and published [12, 13], etc...

In this study, we have numerically investigated electron transport in multi-barrier structures on a graphene layer using the following formalism: The Dirac equation and transfer matrix along with the Landauer-Büttiker approximation. The transmission coefficient and conductance as a function of electron energy were calculated for three generated configurations of the structure.

2 Methodology

The graphene-based structures (see Fig. 1) are described as follows: each structure is characterized by a specific number of barriers with distinct dimensions and heights. In order to generate the G_3 configuration, the structure consists of 4 barriers, each with a width of $W_B = 148$ Åand a height of $V_0 = 0.04$ eV. In the next configuration, G_4, the number of barriers increases to 8, and these barriers are narrower and shorter when compared to those in the G_3 configuration, for instance, with a width of $W_B = 49$ Åand a height of $V_0 = 0.02$ eV. Finally, in the last configuration G_5, the structure consists of 16 barriers with the smallest dimensions, having a width of $W_B = 16$ Åand a height of $V_0 = 0.01$ eV.

The top gate (electrostatic barrier) significantly influences the physical properties of graphene. When an external voltage is applied to graphene through a top gate, an electrostatic potential is generated which acts as an electrostatic barrier for the electrons in graphene. The height of this electrostatic barrier is proportional to the applied voltage due to the direct relationship between the generated electrostatic potential and the electric field induced by the voltage. This electrostatic barrier affects the energy of the electrons and specifically, induces a shift in the Dirac cone, as the energy level of the electrons in graphene is modified by the external potential [5, 7].

Because electrons in graphene behave as relativistic mass zero particles, the Dirac equation can be applied to study their transport properties [14, 20]. To this end, the following formula is used:

$$[v_F(\boldsymbol{\sigma_i}.\boldsymbol{p}) + V_0]\psi = E\psi, \tag{1}$$

where $\boldsymbol{\sigma_i}$ with $i = x, y, z$ is the i^{th} Pauli matrix, v_F is the Fermi velocity and V_0 voltage applied, and $\overrightarrow{p}$ is the momentum.

By solving Eqn. 1, the eigenfunctions and eigenvalues can be computed. To this end, electrons are being considered in the plane wave approximation, permitting to be represented in the barrier regions as:

$$\psi^{\pm}_{q_j}(x, y) = \frac{1}{\sqrt{2}} \begin{pmatrix} 1 \\ v_j^{\pm} \end{pmatrix} e^{\pm i q_{x,j} x + i q_{y,j} y}, \tag{2}$$

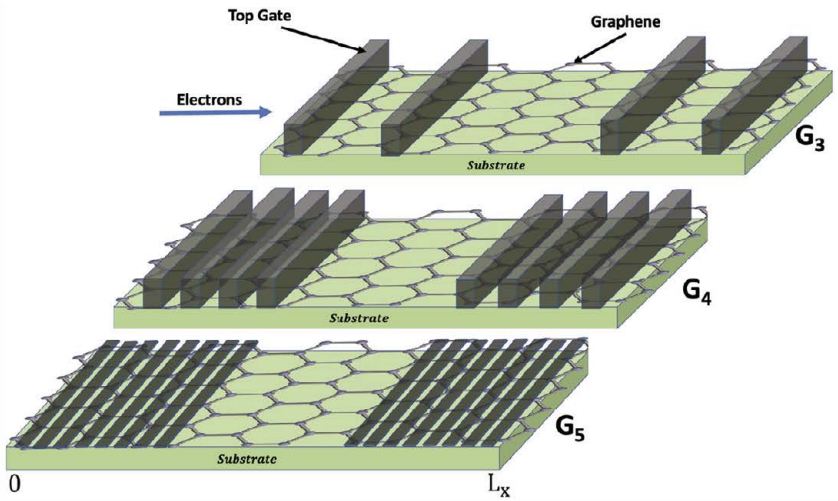

Fig. 1. Illustration of the multi-barrier structure based on graphene, whereas G_3, G_4, G_5 refer to the generated configuration respectively. The electrostatic barriers are represented by top gate.

where $q_j (j = 1, 2, ..)$ is the wave vector and $v_j^{\pm}$ are the wave function components given by:

$$v_j^{\pm} = \frac{E - V_{0,j}}{\hbar v_F (\pm q_{x,j} - i q_{y,j})}. \tag{3}$$

For the case of well regions (No applied voltage), the wave function can be assumed as:

$$\psi_{k_j}^{\pm}(x, y) = \frac{1}{\sqrt{2}} \begin{pmatrix} 1 \\ u_j^{\pm} \end{pmatrix} e^{\pm i k_{x,j} x + i k_{y,j} y}, \tag{4}$$

where $k_j (j = 1, 2, ..)$ is the wave vector and $u_j^{\pm}$ are the wave function components given by:

$$k_j^{\pm} = \pm sign(E) e^{\pm i\theta}. \tag{5}$$

The linear dispersion relation corresponding to the barrier regions where the voltage is applied can be cast into:

$$E - V_0 = \pm \hbar v_F q, \tag{6}$$

where $\pm$ represents electrons and holes, respectively.

Both transmitted (A_{trans}) and incident (A_{incid}) wave amplitudes were computed using the continuity condition of the wave function at each well-barrier interface, along with the conservation of momentum along the y-coordinate ($q_{y,j} = k_y$). Noteworthy, these amplitudes are related through the transfer matrix

method, which provides a systematic framework for analyzing wave propagation in such structures [14]:

$$\begin{pmatrix} A_{incid} \\ B_{incid} \end{pmatrix} = M \begin{pmatrix} A_{trans} \\ 0 \end{pmatrix}, \tag{7}$$

with

$$M(E,\theta) = \begin{pmatrix} M_{11} & M_{12} \\ M_{21} & M_{22} \end{pmatrix}, \tag{8}$$

After computing the transfer matrix, the transmission probability can be directly determined using the following expression:

$$T(E,\theta) = \left| \frac{A_{trans}}{A_{incid}} \right|^2 = \frac{1}{|M_{11}|^2}, \tag{9}$$

where M_{11} is the first element of the transfer matrix.

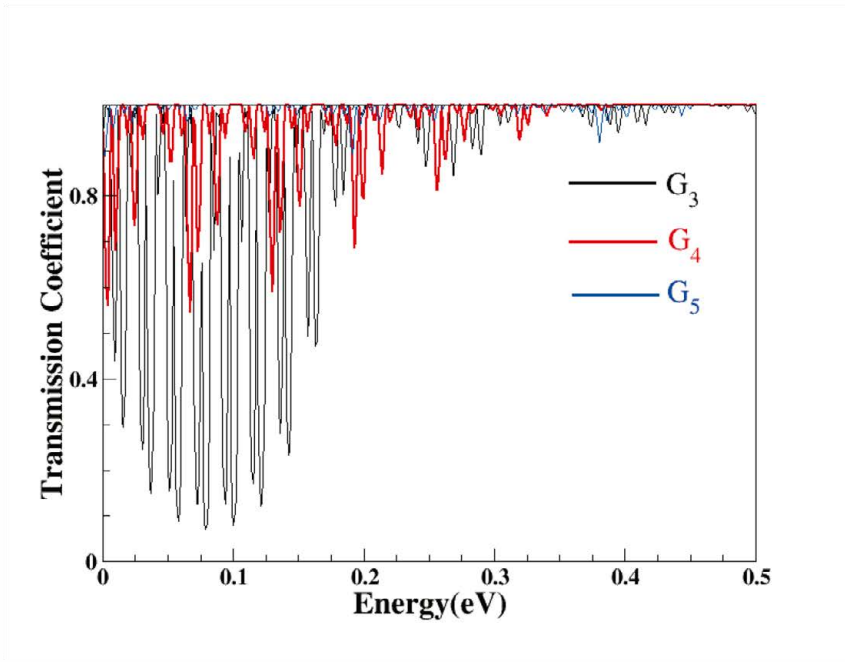

Fig. 2. Transmission coefficient as a function of the energy of electrons for three different generated configurations G_3, G_4, G_5

The calculation of conductance is performed through the transmission coefficient using the Landauer-Büttiker formalism [18]. For a graphene monolayer,

the conductance can be expressed as:

$$G(E_F^*) = \frac{G}{G_0} = \int_{-\frac{\pi}{2}}^{\frac{\pi}{2}} E_F^* T(E_F^*, \theta) \cos\theta d\theta, \tag{10}$$

where $E_F^* = \dfrac{E_F}{V_0}$ is the Fermi energy scaled to the height of the main barrier V_0, $G_0 = \dfrac{2e^2 L_y V_0}{\hbar^2 v_F}$ is the conductance fundamental factor, L_y is the width of the system in the transverse direction y and θ is the angle of incidence of electrons with respect to the propagation along direction x.

Despite the transmission coefficient for a single barrier can be calculated analytically, for multiple barriers, it is computed numerically using the transfer matrix (TM) formalism [22] . Due to its versatility and simplicity, the TM method is widely used to calculate transport properties in quantum systems. One of its key advantages of the TM is its ability to reduce the problem of computing the transmission and reflection coefficients of complex multi-barrier structures by to solving the continuity equations at the interfaces.

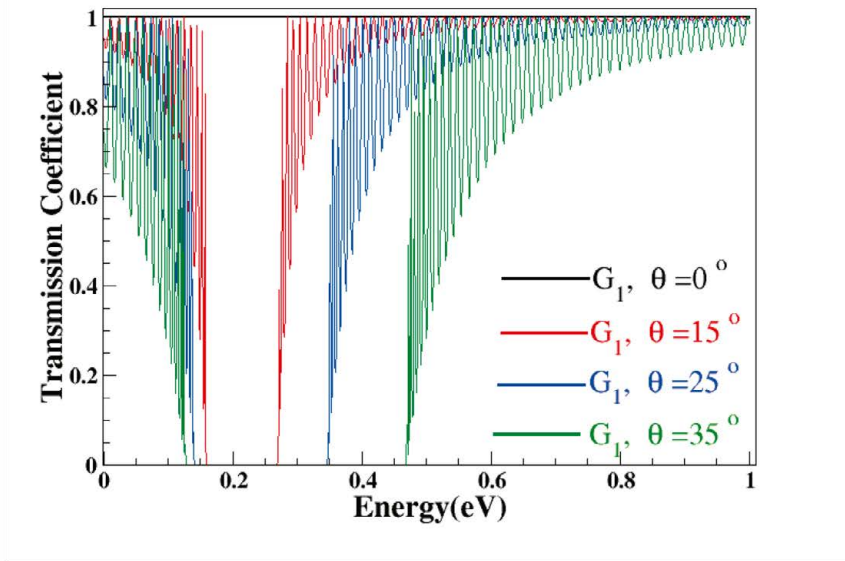

Fig. 3. The transmission coefficient as a function of energy of the first generation with only one barrier, and different angles of incidence.

Furthermore, it is computationally efficient for one-dimensional systems and provides clear physical insights into the scattering and tunneling processes. However, the method has its limitations. It is best suited for systems with one-dimensional potential profiles, and its accuracy decreases for large-scale systems or when dealing with very complex barriers. Such inconveniences result from numerical instabilities associated with the expansion or contraction of waves functions used as a basis to diagonalize the matrix electronic wave equation. From a computational standpoint, the TM may become expensive for systems with a large number of barriers because the size of the matrix product increases and precision errors accumulate. Despite these drawbacks, the method remains a useful tool for studying quantum transport, particularly in systems like graphene or superlattice-based structures.

Considering the above-mentioned comments about the TM formalism, the results are obtained combining an algorithm that simulates the solutions of the Dirac equation and the TM formalism. For instance, this approach is used to calculate the transmission coefficient for different barrier configurations (G_3), (G_4), and (G_5), from where, the conductance is determined, considering the angle of electron incidence $\theta = 15°$.

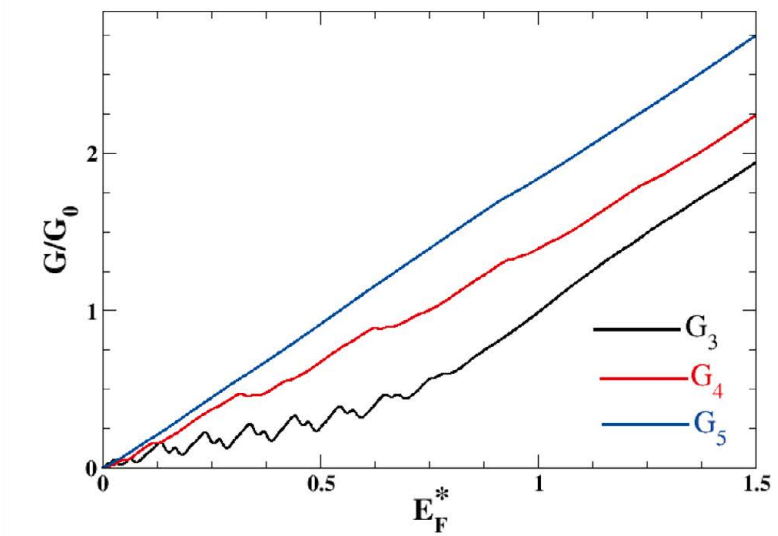

Fig. 4. The conductance as a function of Fermi energy scaled to the height of the barrier for generated configurations G_3, G_4, and G_5 respectively.

3 Results

The results are presented in Figure 2. The transmission coefficient for the G_3 generation shows the probability of electron transmission in the graphene-based structure, passing through four barriers. The transmission curve reveals energies with both maximum and minimum transmission. Noteworthy, the Klein paradox effect (when a Dirac-like particle is incident to a step potential with its height larger than twice the particle's rest mass) is not observed in this case due to the non-normal angles of incidence. As the generated configurations increases from G_3 to G_4 and G_5, an increase in the transmission coefficient is observed. In other words, the energies with maximum transmission also increase. This effect can be explained by the progressive reduction in barrier widths, despite the increase in the number of barriers.

The second case of study is presented in Figure 3. In this case, the transmission coefficient is calculated for a first-generated configuration (G_1), containing only a single barrier. By varying the angle of incidence of the electron, we observe that for $\theta = 0^o$, the Klein paradox is clearly evident, with a perfect transmission. In fact, this effect does not depend on the number or width of the barriers. As the angle of incidence increases, a gap emerges where the transmission energy is zero. With further increases in the angle of incidence, this gap expands, suggesting that the gap has some dependence on the angle of incidence.

The third case investigates the conductance for the G_3, G_4, and G_5 generations. Figure 4 shows the conductance as a function of Fermi energy. For the G_3 generation, it is observed that the conductance increases as the energy increases, clearly demonstrating an energy dependence in this case. As the generation increases, meaning more barriers are added, the conductance also increases for larger generations.

4 Conclusion

In summary, the electronic properties of graphene were investigated numerically considering three cases of interest. It was demonstrated that the energies associated with maximum transmission increase as the number of barriers increases, considering that the barriers in generations G_3 to G_4 become progressively wider. This is clear from results for the transmission coefficient, which show an increasing trend. Additionally, the transmission coefficient was studied for a single barrier with different electron angles of incidence. It was observed that Klein tunneling is present at angles with normal incidence; however, this phenomenon disappears as the incidence angle increases, a result that has been extensively studied by different groups, as discussed in [21]. Additionally, we calculated the conductance for the three mentioned generated configurations (G_3, G_4, and G_5), demonstrating that the conductance increases as the generation increases. A dependence of the conductance on the Fermi energy was also observed. These types of structures serve as a testbed for modulating the band gap, redistributing the density of states, and generating energy regions with an accumulation of energy levels in graphene monolayers. Finally, the TM is a highly useful method, as it

allows complex systems to be represented using simple and combinable matrices. However, it is important to mention that for systems with a large number of matrices barriers, it can become numerically complex, leading to numerical errors that must be addressed in the most effective way possible.

Acknowledgments. This work was supported by SECIHTI Posdoctoral Program (POSDOC). We thank UAN for the facility to use the infrastructure.

Disclosure of Interests. The authors have no competing interests to declare that are relevant to the content of this article.

References

1. William H. Press, et al., *Numerical Recipes: The Art of Scientific Computing*, 3rd ed., Cambridge University Press, 2007, ISBN: 9780521880688, https://www.cambridge.org/core/books/numerical-recipes/0469EC5C31E1D1C6B92EAD82B6349F97.
2. J. L. Martins, F. R. Vukmirovic, A. B. S. A. S. L. G. de Lima, *Computational Materials Science: From Theory to Applications*, Springer, 2011.
3. J. Schoenes, *Computational Methods in Solid State Physics*, Springer, 1987.
4. P. Giannozzi, O. Timings, J. L. G. et al., *QUANTUM ESPRESSO: A modular and open-source software project for quantum simulations of materials*, Journal of Physics: Condensed Matter **21**, 395502 (2009).
5. K. S. Novoselov, A. K. Geim, S. V. Morozov, D. Jiang, Y. Zhang, S. V. Dubonos, I. V. Grigorieva, A. A. Firsov, *Electric field effect in atomically thin carbon films*, Science **306**, 5696 (2004), 666–669.
6. K. S. Novoselov, D. Jiang, F. Schedin, T. J. Booth, V. V. Khotkevich, S. V. Morozov, A. K. Geim, *Two-dimensional atomic crystals*, Proceedings of the National Academy of Sciences **102**, 30 (2005), 10451–10453.
7. M. I. Katsnelson, K. S. Novoselov, A. K. Geim, *Chiral tunnelling and the Klein paradox in graphene*, Nature Physics **2**, 9 (2006), 620–625.
8. B. Huard, J. A. Sulpizio, N. Stander, K. Todd, B. Yang, D. Goldhaber-Gordon, *Transport measurements across a tunable potential barrier in graphene*, Physical Review Letters **98**, 23 (2007), 236803.
9. T. Ma, Ch. Liang, L.-G. Wang, H.-Q. Lin, *Electronic band gaps and transport in aperiodic graphene superlattices of Thue-Morse sequence*, Applied Physics Letters **100**, 25 (2012), 252402, American Institute of Physics.
10. Zh. Zhang, L. H., Zh. Gong, Y. Fan, T. Zhang, H. Chen, *Extend the omnidirectional electronic gap of Thue-Morse aperiodic gapped graphene superlattices*, Applied Physics Letters **101**, 25 (2012), 252104, American Institute of Physics.
11. Y. P. Bliokh, V. Freilikher, S. Savel'ev, F. Nori, *Transport and localization in periodic and disordered graphene superlattices*, Phys. Rev. B **79**, 7 (2009), 075123, American Physical Society, https://link.aps.org/doi/10.1103/PhysRevB.79.075123.
12. J. Zhang, H. Peng, H. Zhang, S. Maruyama, and L. Lin, "The Roadmap of Graphene: From Fundamental Research to Broad Applications," *Advanced Functional Materials*, vol. 32, no. 42, 2022.
13. F. Schwierz, "Graphene Transistors," *Nature Nanotechnology*, vol. 5, pp. 487–496, 2010. DOI: 10.1038/nnano.2010.89.

14. P. Markos, C. M. Soukoulis, *Wave propagation: from electrons to photonic crystals and left-handed materials*, Princeton University Press, 2008.
15. S. Y. Zhou, G.-H. Gweon, A. V. Fedorov, P. N. First, W. A. De Heer, D.-H. Lee, F. Guinea, A. H. Castro Neto, A. Lanzara, *Substrate-induced bandgap opening in epitaxial graphene*, Nature Materials **6**, 10 (2007), 770–775.
16. N. W. Ashcroft, N. D. Mermin, *Solid State Physics*, Harcourt College Publishers, 1976.
17. W. Kohn, L. J. Sham, *Self-Consistent Equations Including Exchange and Correlation Effects*, Physical Review **140**, A1133–A1138 (1965).
18. S. Datta, *Electronic Transport in Mesoscopic Systems*, Cambridge University Press, 1997.
19. S. V. Morozov, K. S. Novoselov, A. K. Geim, *Electron transport in graphene*, Uspekhi Fizicheskikh Nauk **178**, 7 (2008), 776–780, Russian Academy of Sciences, Branch of Physical Sciences.
20. M. Barbier, P. Vasilopoulos, F. M. Peeters, *Extra Dirac points in the energy spectrum for superlattices on single-layer graphene*, Physical Review.
21. M. I. Katsnelson, K. S. Novoselov, and A. K. Geim, "Chiral tunnelling and the Klein paradox in graphene," *Nature Physics*, vol. 2, pp. 620–625, 2006, doi: 10.1038/nphys384.
22. ME Mora, R Pérez, C Sommers *Transfer matrix in one-dimensional problems*, Journal de Physique **46** (7), (1985), 1021-1026.